# Dual-energy computed tomography for the detection of sacroiliac joints bone marrow oedema in patients with axial spondyloarthritis

M. Carotti[1], D. Benfaremo[2], M. Di Carlo[3], L. Ceccarelli[3], M.M. Luchetti[2], P. Piccinni[1], A. Giovagnoni[1], F. Salaffi[3]

*[1]Radiology Clinic, Dipartimento di Scienze Cliniche Specialistiche e Odontostomatologiche, Università Politecnica delle Marche;*
*[2]Medical Clinic, [3]Rheumatology Clinic, Dipartimento di Scienze Cliniche e Molecolari, Università Politecnica delle Marche, Ancona, Italy.*

## Abstract

### Objective

*To investigate the diagnostic performance of dual-energy computed tomography (DECT) in detection bone marrow oedema (BME) in patients with sacroiliitis associated with axial spondyloarthritis (axial SpA).*

### Methods

*Patients with axial SpA according to the ASAS criteria underwent DECT and 1.5-T magnetic resonance imaging (MRI). DECT was post-processed for generating virtual non-calcium (VNCa) images. The presence of abnormal bone marrow attenuation was scored on DECT VNCa images and MRI using a four-point classification system: 0-1 = absent or non-significant oedema, 2 = oedema present in a third of the articular surface, 3 = oedema present in 2/3 of the articular surface, 4 = diffuse oedema throughout the articular surface. Diagnostic accuracy values for BME were calculated for DECT images (quantitative assessment) by using receiver operating characteristic (ROC) curves analysis, applying MRI as gold standard.*

### Results

*Eighty sacroiliac joints from 40 axial SpA patients were included for study analysis, and 36 sacroiliac joints (45%) were classified as having BME at MRI and compared to DECT. Sensitivity, specificity, and positive likelihood ratio (LR+) in the identification of BME at DECT were 90.0%, 92.8%, and 12.6 respectively. Negative LR was 0.11, positive predictive value 93.1%, and negative predictive value 89.7%. The area under the curve (AUC) was 0.953 in the differentiation of the presence of BME. A cut-off value of -1.6 HU (Youden's index = 0.828) yielded a sensitivity of 90.0% and specificity of 92.8%, with an LR+ of 12.6, in the detection of BME in the sacroiliac joints.*

### Conclusion

*DECT VNCa images had good diagnostic performance in the evaluation of the extent of BME in patients with sacroiliitis associated with axial SpA.*

### Key words

dual-energy computed tomography, magnetic resonance imaging, bone marrow oedema, sacroiliitis, axial spondyloarthritis

*Marina Carotti, MD*
*Devis Benfaremo, MD*
*Marco Di Carlo, MD*
*Luca Ceccarelli, MD*
*Paola Piccinni, MD*
*Michele Maria Luchetti, MD*
*Andrea Giovagnoni, MD*
*Fausto Salaffi, MD, PhD*

*Please address correspondence to:*
*Marco Di Carlo,*
*Clinica Reumatologica,*
*Università Politecnica delle Marche,*
*Ospedale Carlo Urbani,*
*60035 Jesi (AN), Italy.*
*E-mail: dica.marco@yahoo.it*

*Received on June 7, 2020; accepted in revised form on October 27, 2020.*



*ORCID iD:*
*M. Carotti: 0000-0001-6562-180X*
*D. Benfaremo: 0000-0002-9867-2360*
*M. Di Carlo: 0000-0002-0906-4647*
*L. Ceccarelli: 0000-0002-0510-0970*
*A. Giovagnoni: 0000-0002-5264-652X*
*F. Salaffi: 0000-0002-3794-6831*

*Competing interests: none declared.*

## Introduction

The sacroiliac joints are involved in most cases of axial spondyloarthritis (axial SpA), with sacroiliitis usually being the first manifestation (1). The new Assessment of SpondyloArthritis international Society (ASAS) criteria (2), which include magnetic resonance imaging (MRI) findings, facilitate early diagnosis and assessment of treatment response because of the ability of MRI to detect active inflammation (3). However, because of some inherent technical limitations and contraindications, it is not always possible to use MRI in the routine diagnosis of sacroiliitis. Other disadvantages of the MRI are long execution times, which limit the availability of the technique.

Dual energy computed tomography (DECT) is a revolutionary imaging method that enables detection of traumatic bone marrow oedema (BME) (4), plasma cell infiltration of bone marrow (5), and whose use has instead increased over the last decade in many other clinical applications. Dual source scanners are equipped with two x-ray tubes, which operate at different voltages (70 kVp and 150 kVp) allowing the simultaneous acquisition of images at these two different energy levels. DECT is superior to single energy CT, due to its ability to differentiate materials based on the different degrees of absorption and attenuation of the x-ray beam which, in turn, depend on the atomic number of the various components under examination. Comparing the different attenuation levels at high and low energy, respectively, DECT allows the decomposition of materials using specific post-processing algorithms (6).

In the last decade, several clinical applications have been reported for DECT (7). The principal applications in musculoskeletal imaging include: 1) detection of urate crystals in patients with gout and with asymptomatic hyperuricemia; 2) BME detection, *e.g.* in the case of trauma, algoneurodystrophy or inflammation (osteitis); 3) characterisation of collagenous structures, such as tendons, ligaments and intervertebral disks; 4) minimisation of metal prosthesis beam-attenuating artifacts.

For the detection of BME, a dedicated software removes calcium of trabecular bone, the so-called "virtual non-calcium subtraction" (VNCa technique), creating VNCa images. Increased water content or cellular components, such in multiple myeloma or bone metastases, in the bone marrow can be visualised on VNCa images. Using colour-coded, DECT VNCa application, oedema can be depicted as colour imaging grey-scale overlay or even 3D. DECT, in addition of colour-coded VNCa images to standard CT, is able to simultaneously visualise BME and minor structural lesions in the sacroiliac joints of patients with axial SpA (8).

According to the ASAS classification criteria for axial SpA (2, 9), the presence of BME on MRI STIR sequence is usually sufficient for the definition of active sacroiliitis. The T1 sequence after application of gadolinium might give additional information in unclear cases and/or for the exclusion of possible artefacts, although it is generally not needed. Other inflammatory lesions such as synovitis, enthesitis or capsulitis are certainly compatible with axial SpA sacroiliitis, but without the simultaneous presence of typical BME they were not regarded as sufficiently specific to justify a diagnosis of sacroiliitis.

MRI is also capable of depicting structural lesions, such as erosions, fat lesion, sclerosis, bone bridges and ankylosis, which reflect previous inflammation, however the sole presence of these lesions without concomitant BME/osteitis does not suffice for the definition of a positive MRI. Nevertheless, the recognition of structural lesions on T1-weighted MRI contributes significantly to its diagnostic utility in early axial SpA (10, 11).

This study has two objectives.

First, we aim to investigate the diagnostic performance of a third generation DECT scanner in detection BME in patients with sacroiliitis, associated with axial SpA, by using MRI as the standard of reference.

Second, we try to identify the optimal cut-off value of DECT in the differentiation of the presence of BME from no oedema.

## Materials and methods

*Patients*

Between February 2018 and March 2020, 40 patients with axial SpA, referred for MRI because of clinical suspicion of sacroiliitis were enrolled in the Rheumatology Clinic of the Carlo Urbani Hospital in Jesi (Ancona, Italy) and in the Medical Clinic of the Umberto I-G.M.Lancisi-G. Salesi Hospital of Ancona (Italy) and evaluated for the presence of abnormal marrow attenuation on DECT.

The inclusion criteria were: 1. adult patients with a diagnosis of axial SpA according to the ASAS Classification Criteria (2), 2. patients with a recently performed MRI examination of the sacroiliac joints at the Department of Radiological Sciences of the Umberto I-G.M.Lancisi-G. Salesi of Ancona (Italy) within the 30 days preceding the DECT examination, 3. the non-introduction of new treatments (biological or non-steroidal anti-inflammatory drugs) and the non-execution of switches between biological drugs between MRI and DECT, 4. patients that signed a written informed consent. The exclusion criteria were: 1. refusal to carry out the examination according to the study protocol, 2. pregnancy (women of childbearing potential were requested to perform a pregnancy test before informed consent), 3. patients with previous fractures of the pelvic bones, 4. patients with previous coxo-femoral prosthetic surgery, 5. patients with known onco-hematological neoplasms. All patients agreed to participate in the study, signed informed consent, and the procedures conducted in the study were approved by the local Ethics Committee and were in accordance with the Helsinki Declaration of 1975 and its later amendments.

*DECT protocol*

All CT examinations were performed using a 384 (192Å~2)-slices third generation Dual Source CT scanner (SOMATOM Force CT; Siemens Healthineers, Forchheim, Germany) installed at the Department of Radiological Sciences of the Umberto I-G.M.Lancisi - G. Salesi Hospital of Ancona (Italy). The scanner is equipped with two x-ray tubes (tube A with low kilovoltage; tube B with high kilovoltage), and two corresponding detectors were installed with an angular offset of 95. All patients were examined in supine position, within 30 days of the MRI imaging. Cranio-caudal CT was performed with the same dual-energy protocol: 90 kV for tube A and 150 Sn kV for tube B, quality reference mAs 150 for tube A and 120 for tube B, dose modulation software: CareDose4D® (Siemens®), detector collimation: 128x0.6 mm, pitch: 0.6, rotation time 0.5 s.

No intravenous contrast agent was used. From the DECT acquisition, three different sets of images were obtained: low KVp images, high KVp images and images obtained from the average of the two voltages, called "mixed". The mixed series were retro-reconstructed with a high spatial algorithm at 0.6 mm (bone filter) on which multi parametric reconstruction (MPR) are performed in the sagittal, coronal and oblique planes. Maximum effective radiation dose to the sacroilic joint from DECT was less than 4 mSv, with a mean of 3.35±1.18 mSv, equivalent to one third of the conventional CT (mean of 10.72 mSv).

*Post-processing and semi-quantitative and quantitative analysis of DECT*

Two CT data sets were transferred to a workstation equipped with DECT post-processing software (Syngo Dual Energy, v. VA11A; Siemens Healthcare, Erlangen, Germany) for image analysis. The software can characterise and differentiate various chemical elements, through the use of three material decomposition algorithm for bone mineral, yellow bone marrow, and red bone marrow. Calcium is removed in trabecular bone by using the VNCa subtraction process to create VNCa images where bone marrow can be assessed without superposition. VNCa images were displayed as colour-coded overlay maps merged with weighted average CT images. The colour-coded evaluation ranged from pink/blue (fat), green (water/BME) to yellow (increasing red marrow/blood content). Additionally, axial, coronal and sagittal multiplanar reconstructions of the mixed VNCa images were acquired for semi-quantitative and quantitative image reading (slice thickness 1 mm, increment 1 mm). Visual analysis of colour-coded images and quantitative region of interest (ROI)-based density measurements were used to detect sacroiliac joint BME (Figs. 1-2).

The CT scan images of both the groups were reviewed by two radiologists with experience of 20 and 5 years, respectively, in musculoskeletal image interpretation on the PACS independently. The radiologists were blinded to the clinical findings, MRI results and diagnosis. The cases were mixed prior to allotting to the radiologists. A visual semiquantitative score based on the extent of BME was assigned in the affected area, using MRI T2-weighted fat suppression as the reference standard: 0–1 = absent or non-significant oedema (oedema involving less than 1/3 of the sacroiliac joint), 2 = oedema present in a third of the articular surface, 3 = oedema present in 2/3 of the articular surface, 4 = diffuse oedema throughout the articular surface. For quantitative analysis a ROI was positioned manually on the oedema zone marked as green background on the colour-coded images to obtain DECT VNCa numbers. With the consent of the two operators, three ROIs were manually positioned for each side of the sacroiliac joints (for a total of 12 ROIs) in the subchondral region of the proximal, middle and distal thirds of each joint surface, respectively. All the positioned ROIs had an area of 0.1 $cm^2$. The dedicated software allows the precise calculation of the attenuation values (in HU units) in the three ROIs for each articular surface of sacroiliac joints (Fig. 1).

*MRI protocol*

All the sacroiliac joints MRI were performed on a 1.5T MRI (Achieva Philips Medical Systems, Best, the Netherlands) machine with a 16-channel "dStream torso coil" coil. The protocol included turbo spin echo (TSE) axial T1, axial short-tau-inversion-recovery (STIR), TSE axial T2, TSE coronal T1, coronal STIR, TSE coronal T2, fast field echo FFE axial T2, coronal TSE T1, para-axial of the sacred T1, para-axial of the sacred STIR, para-coronal of the sacred T1, para-coronal of the sacred STIR.

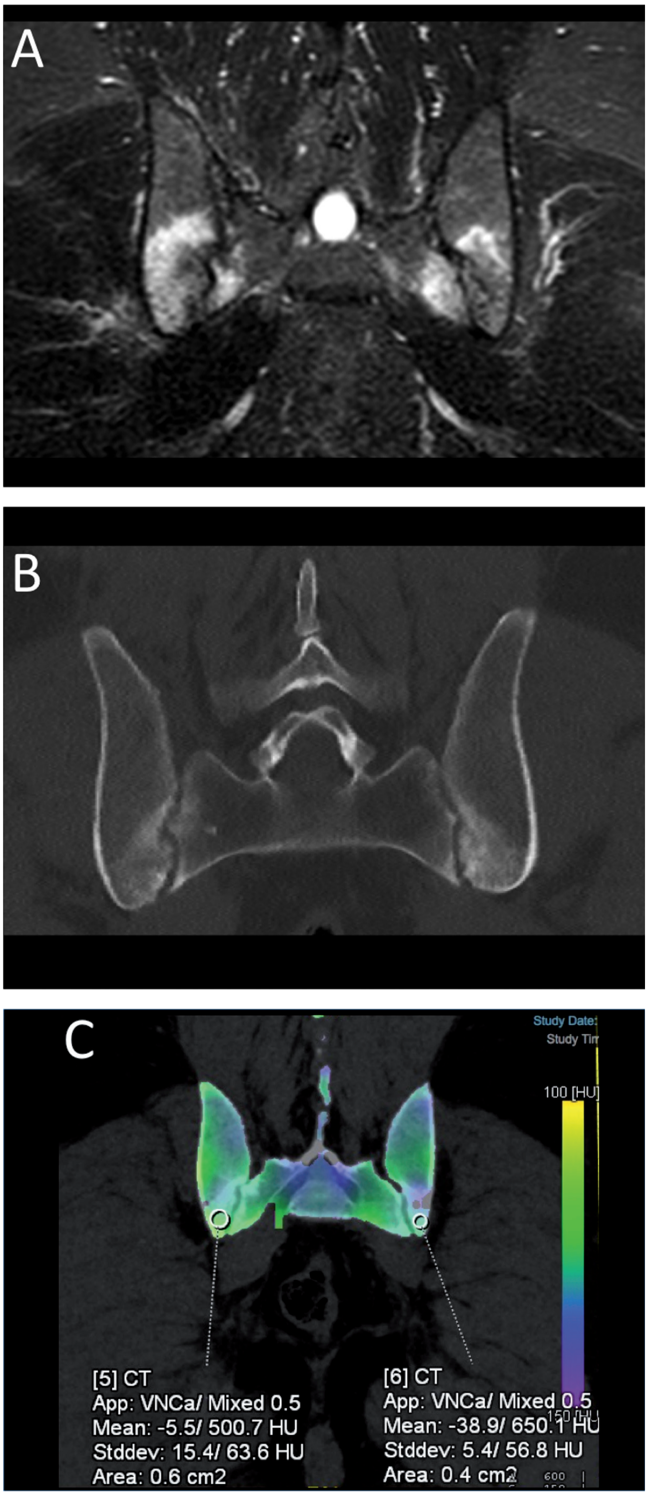


**Fig. 1.** Patient with axial spondyloarthritis.
**A**: Short tau inversion recovery magnetic resonance image in the semicoronal plane demonstrating extensive bone marrow oedema in both iliac and sacral subchondral bone, indicating active sacroiliitis.
**B**: Computed tomography, semicoronal multiplanar reformatted greyscale image shows signs of structural change. Erosions of both iliac and sacral cortical bone leading to an appearance of widening of the joint space and bilateral iliac subcondral sclerosis may be observed.
**C**: Semicoronal multiplanar reformatted colour-coded dual-energy computed tomography virtual non-calcium image reveals bone marrow signal (depicted in green) involving both sacroliliac joints, corresponds to bone marrow oedema on magnetic resonance imaging in **A**. The dedicated software also allows the precise calculation of the attenuation values in the region of interest to be referred to oedema, more evident on the right side.

*Semiquantitative analysis of MRI*

The 0–4 semiquantitative score applied for DECT images, depending on the extent of BME, was assigned in the affected area by each operator (the same operators that scored DECT images), independently, also on STIR image. The semiquantitative score was applied on iliac and sacral surfaces of each sacroiliac joint. In cases of intra-observer and inter-observer disagreement, consensus ranking was obtained.

*Statistical analysis*

The data were processed with the MedCalc Statistical Software, v. 19.0 (Ostend, Belgium), for Windows XP. General descriptive statistics were summarised using numbers and percentages for categorical variables, while mean ± standard deviation (SD) and median were utilised for continuous variables. The differences in proportions between the groups were compared using a chi-square or Fisher's exact test where appropriate. Continuous variables were compared using the Mann-Whitney U-test among categories of grouped variables, and the degree of correlation between the variables was calculated using Spearman's rho correlation coefficients.

The intra-observer and inter-observer agreement was calculated with Cohen's weighted kappa method in the semi-quantitative evaluation of the scores assigned in DECT.

The accuracy of DECT for the detection of BME compared to MRI (applied as external criterion) was analysed using the receiver operating characteristics (ROC) curve analysis. The ROC curves were plotted to determine the area under the curve (AUC), the sensitivity, the specificity and the likelihood ratios, calculated at the optimal cut-off (identified in the Youden's index). The AUC was used to evaluate the overall diagnostic performance of the test. According to Swets, area under the curve (AUC) values from 0.5 to 0.7 represent poor accuracy, those from 0.7 to 0.9 are moderate and those above 0.9 represent high accuracy (12). We computed ROC curves on 1000 bootstrapped samples, using non-parametric resampling and the bias-corrected and accelerated method to compute 95% confidence intervals (CIs). The level of significance was set at $p<0.05$ for all the analyses.

## Results

Eighty sacroiliac joints in 40 patients with axial SpA (30 males and 10 females) were included for study analysis. The mean (SD) age of patients was of 48.6 (12.3) years, with a mean (SD) disease duration of 5.5 (2.9) years, and a mean (SD) C-reactive protein (CRP) of 3.0 (2.5) mg/dl.

23 patients (57.5%) were taking biological therapy, represented by adalimumab (8 patients, 20%), etanercept (6 patients, 15%), golimumab (4 patients, 10%), certolizumab pegol (3 patients,

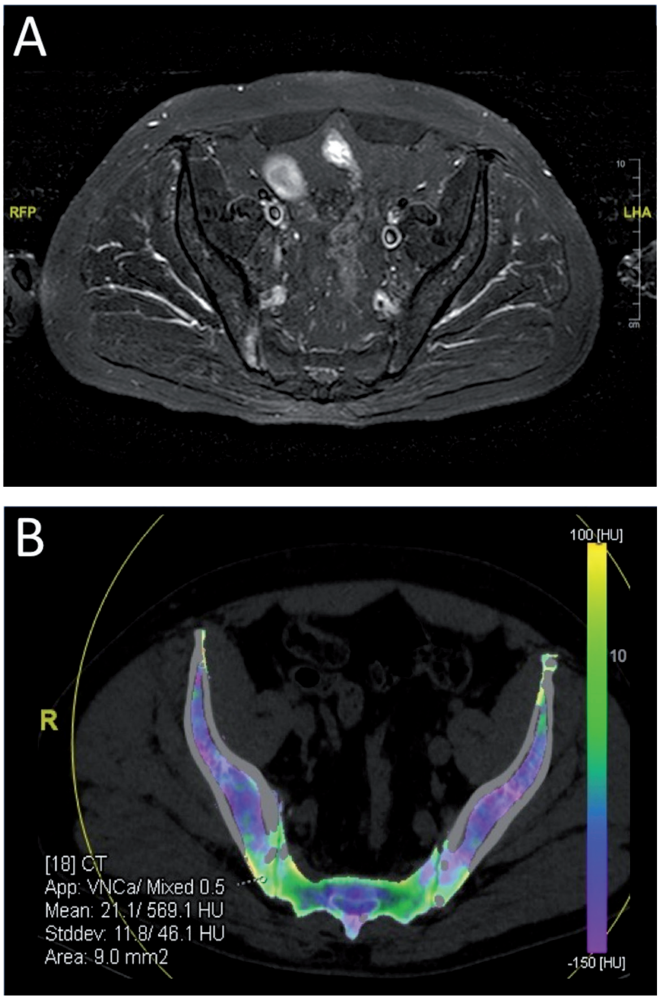


**Fig. 2.** Patient with spondyloarthritis.
**A**: Short tau inversion recovery magnetic resonance image in the axial plane demonstrating bone marrow oedema in right iliac subcondral bone, indicating active sacroiliitis.
**B**: Axial multiplanar reformatted colour-coded dual-energy virtual non-calcium image reveals bone marrow signal (depicted in green) involving sacroliliac joints, corresponds to bone marrow oedema on the magnetic resonance image. The dedicated software also allows the precise calculation of the attenuation values in the region of interest (ROI) to be referred to oedema, on the right side.

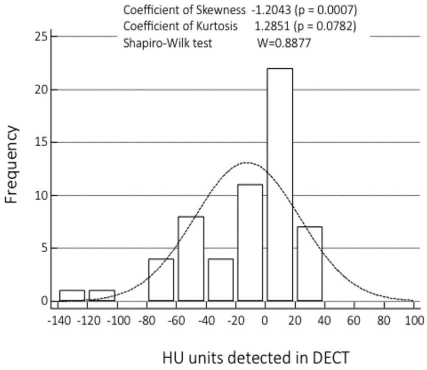


**Fig. 3.** Percentage distribution of the values of Hounsfield units detected in dual-energy computed tomography.

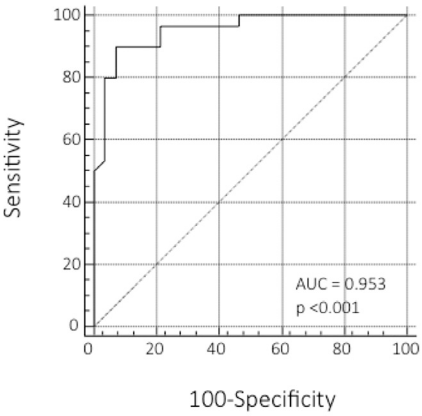


**Fig. 4.** Receiver operating characteristic (ROC) curve calculated for Hounsfield units (derived from dual-energy computed tomography virtual non-calcium images) in the detection of bone marrow oedema. Area under the ROC curve is 0.953 (standard error 0.0257 and 95% CI 0.863–0.991).

7.5%), and secukinumab (2 patients, 5%). Three patients (7.5%) were taking sulfasalazine, nine patients (22.5%) were taking etoricoxib 90 mg/day at stable dosage between MRI and DECT, and five patients (12.5%) were not taking any drug treatment.
There were no differences between males and females with regard to age and disease duration, whereas male subjects showed a higher CRP level ($p$=0.02) and a lower attenuation (HU units) ($p$=0.01), compared to females. The descriptive analysis of the values of HU units detected in CT is reported in Figure 3, where a non-parametric distribution is highlighted.
Thirty-six (45%) of the 80 sacroiliac joints available for analysis were classified as having BME at MRI. MRI was used to classify 16 sacroiliac joints as having mild BME (score 2), 11 as having moderate BME (score 3), and 9 as having severe BME (score 4), based on the extent of BME in the iliac and sacral surface of each sacroiliac joint.
The weighted kappa in assessing the BME presence between the two operators (inter-observer agreement) was 0.815, with a standard error of 0.04, and a 95% confidence interval (CI) 0.731–0.892. The intra-observer agreement was 0.897, with a standard error of 0.05, and a 95% CI 0.781–0.923.
HU in DECT semiquantitive scoring system demonstrated significative differences between the different grades, compared to MRI ($p$<0.0001, Kruskal-Wallis test).
The accuracy of the DECT in the detection of BME, showed an AUC of 0.953 (standard error 0.0257, 95% CI 0.863–0.991) in the differentiation of the presence of BME from no oedema (Fig. 4). The cut-off value of -1.6 HU (Youden's index = 0.828) yielded a sensitivity of 90.0% (95% CI 73.5–97.9), a specificity of 92.8% (95% CI 76.5–99.1), a LR+ of 12.6 (95% CI 3.3–48.2), a LR- of 0.11 (95% CI 0.04–0.3) (Table I), a positive predictive value of 93.1% (95% CI 77.9–98.1), and a negative predictive value of 89.7% (95% CI 74.7–96.2).

## Discussion

In this study we have demonstrated the usefulness of DECT in the identification of BME in axial SpA sacroiliitis. We used a third generation DECT with VNCa subtraction protocol for the detection of sacroiliac joints BME, using MRI as gold standard. Although there was no histopathological correlation, the advantages of DECT, such as high spatial resolution and image reconstruction technology, may improve the detectability of sacroiliac joints BME. BME is indispensable to establish the

**Table I.** Criterion values and coordinates of the receiver operating characteristic curve for the Hounsfield units indicative of the presence of significant bone marrow oedema at dual-energy computed tomography.

| Criterion | Sensitivity | 95% CI | Specificity | 95% CI | LR+ | 95% CI | LR- | 95% CI |
|---|---|---|---|---|---|---|---|---|
| >-39 | 100.00 | 88.4 - 100.0 | 53.57 | 33.9 - 72.5 | 2.15 | 1.4 - 3.2 | 0.00 | 0.005 - 0.2 |
| >-31 | 96.67 | 82.8 - 99.9 | 53.57 | 33.9 - 72.5 | 2.08 | 1.4 - 3.1 | 0.06 | 0.009 - 0.4 |
| >-11 | 96.67 | 82.8 - 99.9 | 78.57 | 59.0 - 91.7 | 4.51 | 2.2 - 9.2 | 0.04 | 0.006 - 0.3 |
| >-10 | 90.00 | 73.5 - 97.9 | 78.57 | 59.0 - 91.7 | 4.20 | 2.0 - 8.6 | 0.13 | 0.04 - 0.4 |
| >-1.6* | 90.00 | 73.5 - 97.9 | 92.86 | 76.5 - 99.1 | 12.60 | 3.3 - 48.2 | 0.11 | 0.04 - 0.3 |
| >5 | 80.00 | 61.4 - 92.3 | 92.86 | 76.5 - 99.1 | 11.20 | 2.9 - 43.1 | 0.22 | 0.1 - 0.4 |
| >5.85 | 80.00 | 61.4 - 92.3 | 96.43 | 81.7 - 99.9 | 22.40 | 3.2 - 154.8 | 0.21 | 0.1 - 0.4 |
| >11 | 53.33 | 34.3 - 71.7 | 96.43 | 81.7 - 99.9 | 14.93 | 2.1 - 105.3 | 0.48 | 0.3 - 0.7 |

CI: confidence intervals; LR+ : positive likelihood ratio; LR- : negative likelihood ratio; *: optimal cut-off point.

**Table II.** Advantages and disadvantages of computed tomography (CT), dual-energy computed tomography (DECT) and magnetic resonance imaging (MRI).

| | Advantages | Disadvantages |
|---|---|---|
| **CT** | Short acquisition time, widespread availability, and a relatively low cost | Radiation exposure |
| | Best procedure to evaluate structural damage | The inability of conventional single-energy CT to depict bone marrow oedema (the early stage of active inflammation), |
| **DECT** | The possibility of simultaneously assessing osseous structures and changes in bone marrow. | Radiation exposure |
| | | Dual energy CT is not yet widely used or is unknown, |
| | Modern DECT is not associated with higher radiation exposure than classical CT | Current poor availability of DECT scanners. |
| **MRI** | Is the most sensitive method to evaluate the bone marrow space and any oedematous changes | Limited availability, costs, investigation time, patient compliance |
| | | Relatively high costs and the high patient compliance |
| | | More time consuming and expensive than the other procedures. |
| | | Patient contraindications (*e.g.* cardiac pacemaker/ICD). |

diagnosis of active sacroiliitis. An important advantage of DECT is provided by automated volume evaluation software, which allows for quantification of BME. This measure shows high intra- and inter-reader reproducibility. Ours is not the first work to assess the potential of DECT in sacroiliitis. Wu and coworkers investigated 47 patients with axial SpA with DECT (8). Two independent readers evaluated all sacroiliac joints for the presence of abnormal marrow attenuation on dual-energy VNCa images, using a four-point classification system (0, no oedema; 1, mild oedema; 2, moderate oedema; 3, severe oedema). The AUC was 0.930 for reader 1 and 0.910 for reader 2 in differentiation of the presence of BME. They found that the optimal cut-off point value was -33.4 and -42.35 HU for reader 1 and 2, respectively. The results of our study showed that DECT has an overall sensitivity of 90.0%, specificity of 92.8%, and the optimal cut-off value of -1.6 HU. More recently, Chen and collaborators (13), evaluated the feasibility and diagnostic accuracy of DECT for the detection of BME in 40 patients suspected for sacroiliitis, with a good interobserver agreement, moderate sensitivity, and high specificity. Overall inter-reader agreement for visual image reading of BME on VNCa images was good ($\kappa$=0.70). The sensitivity and specificity of BME detection by DECT were 65.4% and 94.2% on the quadrant level and 81.3% and 91.7% on the patient level. ROC analyses revealed AUCs of 0.90 and 0.87 for CT numbers in the ileum and sacrum, respectively. Cut-off values of -44.4 HU (for iliac quadrants) and -40.8 HU (for sacral quadrants) yielded sensitivities of 76.9% and 76.7% and specificities of 91.5% and 87.5%, respectively. The differences in HU cut-offs for the presence of significant oedema are different between the various studies, including ours. The discrepancies of these results may be due to different scanners, different kilovoltage settings, and different postprocessing algorithms (14, 15). A certain influence could also depend on the population studied, given the high prevalence of the lesion in our case study. This aspect currently limits the generalisability of cut-offs proposed. The semi-quantitative interpretation of MRI oedema can also be interpreted differently depending on the reader. However, in the same context and with the same machines, a Cohen's weighted kappa coefficient greater than 0.8 is indicative of an excellent agreement between different observers, which independently assessed both MRI and DECT images. The small differences detected in the interpretation of post-processing colour maps on Syngo Via® can be ascribed to the relative poor experience with this new post-processing method.

The results of our study highlight the usefulness of DECT for the evaluation of axial SpA patients, especially for individuals who have contraindications to the MRI exam. Moreover, the possibility of obtaining at the same time information on the extent of acute inflammation and the chronic structural damage of the sacroiliac joints is extremely convenient.

Recently, the ASAS MRI Working Group updated and further validated the definitions of sacroiliac joints lesions (16), emphasising the unavoidability of BME for the definition of active sacroiliitis but also underlining the need to investigate chronic damage in terms of erosions and sclerosis. In fact, the simple detection of BME is not accurate for the definition of sacroiliitis and structural lesions occur almost as frequently as inflammatory lesions. In a recent study, Baraliakos and coworkers demonstrated that inflammatory and fatty MRI lesions suggestive of axial SpA may occur with a high frequency in the general population (17, 18). For example, BME of the sacroiliac joints was found in 17% of healthy subjects. This observation underlines the need to take into account not only BME but also bone structural lesions, as well as clinical features, in the evaluation of subjects with a suspicion of axial SpA. Conventional single-energy CT is able to detect structural damage, like minor erosion of sacroiliac joints in patients with axial SpA, but does not document BME, which is characteristic in the early stage of active inflammation in patient with axial SpA. In this regard, DECT appears to be a new promising tool for the evaluation of sacroiliac joints in these subjects. The VNCa technique, in fact, allows the identification of BME with a good accuracy, with the added value of an overall better accuracy of the standard CT scan for the evaluation of structural damage, such as erosions and sclerosis. Of note, structural lesions can also be visualised by MRI, but its reliability for the detection of erosions is limited. Moreover, CT has the advantage of being less expensive and requiring shorter examination times (about 10 seconds) than MRI, with consequent better acceptability from both decision-makers and patients. Last, CT is usually more widely available than MRI. Easy access to the technology is important for making an early diagnosis (Table II).

Therefore, numerous pitfalls, which can cause false-positive results, have to be recognised; in particular, it appears difficult to evaluate areas of bone marrow immediately adjacent to cortical bone, sclerotic bone or gas due to potential artifacts (19, 20).

Results from our study support the hypothesis that DECT with reconstruction of VNCa images has enabled both qualitative (visual) and quantitative analysis of BME of sacroiliac joints in study participants with axial SpA, with a precision comparable to that of MRI. Although DECT provides invaluable information in the identification of BME in axial SpA sacroiliitis, the exposure to ionising radiation is of concern with CT-based imaging. The radiation exposure required for DECT depends on the technology used (21). Dose can also be reduced in both single-source and dual-source DECT by applying iterative reconstruction techniques. The radiation dose of a DECT scan lies between 0.1–0.5 mSv per scanned region (*e.g.* 0.5 mSv for both hands and wrists) with a total dose for all scanned peripheral joints ranged from 2 to 3 mSv, which corresponds to the average annual natural background radiation dose (2.4 mSv) (22, 23).

Besides the different technologic approaches to DECT, technologic strategies that allow dose reduction include tube current modulation, iterative reconstruction techniques, and new detector application-specific integrated circuits integrating photodiode and analogue digital converters. These features offer special benefits for DECT because the contrast-to-noise ratios is improved in both half-dose acquisitions with the two energy spectra, so the gain in dose efficiency is even greater than in single-energy CT (21).

Other imaging modalities using radiation are being experimented in axial SpA, including positron emission tomography, whose potential applications should be verified with wider experiences (24).

Finally, there is still a debate on the real meaning of BME in certain circumstances, *i.e.* whether it actually always represents an expression of disease activity (25).

Finally, mention should be made of the limitations of the study. First, the monocentric recruitment on a small number of patients. Second, only affected subjects with a high prevalence of the lesion were studied. To achieve greater validity of the method, DECT will in future have to be studied in case studies with control groups that also include healthy subjects. Thirdly, DECT is a method currently available from a few regional reference structures.

In conclusion, our data confirms the potential of DECT for the detection of BME of the sacroiliac joints in patients affected by axial SpA, in which acute inflammation and chronic damage often occur simultaneously. This new method appears to be useful, not only in the diagnostic phase, but also for objective monitoring of the disease process and in the management of patients with axial SpA.

## References


1. BRAUN J, BOLLOW M, SIEPER J: Radiologic diagnosis and pathology of the spondyloarthropathies. *Rheum Dis Clin North Am* 1998; 24: 697-735.
2. RUDWALEIT M, JURIK AG, HERMANN KG *et al.*: Defining active sacroiliitis on magnetic resonance imaging (MRI) for classification of axial spondyloarthritis: a consensual approach by the ASAS/OMERACT MRI group. *Ann Rheum Dis* 2009; 68: 1520-7.
3. NAVALLAS M, ARES J, BELTRÁN B, LISBONA MP, MAYMÓ J, SOLANO A: Sacroiliitis associated with axial spondyloarthropathy: new concepts and latest trends. *Radiographics* 2013; 33: 933-56.
4. PACHE G, KRAUSS B, STROHM P *et al.*: Dual-energy CT virtual noncalcium technique: detecting posttraumatic bone marrow lesions – feasibility study. *Radiology* 2010; 256: 617-24.
5. KOSMALA A, WENG AM, HEIDEMEIER A *et al.*: Multiple myeloma and dual-energy CT: diagnostic accuracy of virtual noncalcium technique for detection of bone marrow infiltration of the spine and pelvis. *Radiology* 2018; 286: 205-13.
6. AGOSTINI A, BORGHERESI A, MARI A *et al.*: Dual-energy CT: theoretical principles and clinical applications. *Radiol Med* 2019; 124: 1281-95.
7. CAROTTI M, SALAFFI F, BECI G, GIOVAGNONI A: The application of dual-energy computed tomography in the diagnosis of musculoskeletal disorders: a review of current concepts and applications. *Radiol Med* 2019; 124: 1175-83.
8. WU H, ZHANG G, SHI L *et al.*: Axial spondyloarthritis: dual-energy virtual noncalcium ct in the detection of bone marrow edema in the sacroiliac joints. *Radiology* 2019; 290: 157-64.
9. KOUGKAS N, AVGOUSTIDIS N, REPA A, BERTSIAS G, ESKITZIS A, SIDIROPOULOS P:

The value of the 2011 ASAS classification criteria in patients with Spondyloarthritis and the prognosis of non-radiographic axial Spondyloarthritis: data from a large cohort of a tertiary referral hospital. *Mediterr J Rheumatol* 2019; 30: 51-3.
10. WEBER U, LAMBERT RG, PEDERSEN SJ, HODLER J, ØSTERGAARD M, MAKSYMOWYCH WP: Assessment of structural lesions in sacroiliac joints enhances diagnostic utility of magnetic resonance imaging in early spondylarthritis. *Arthritis Care Res* (Hoboken) 2010; 62: 1763-71.
11. WEBER U, ØSTERGAARD M, LAMBERT RG, MAKSYMOWYCH WP: The impact of MRI on the clinical management of inflammatory arthritides. *Skeletal Radiol* 2011; 40: 1153-73.
12. SWETS JA: Measuring the accuracy of diagnostic systems. *Science* 1988; 240: 1285-93.
13. CHEN M, HERREGODS N, JAREMKO JL *et al.*: Bone marrow edema in sacroiliitis: detection with dual-energy CT. *Eur Radiol* 2020; 30; 3393-400.
14. PETRITSCH B, KOSMALA A, WENG AM *et al.*: Vertebral compression fractures: third generation dual-energy CT for detection of bone marrow edema at visual and quantitative analyses. *Radiology* 2017; 284: 161-8.
15. GUGGENBERGER R: Dual-energy CT in the detection of bone marrow edema in the sacroiliac joints: is there a case for axial spondyloarthritis?. *Radiology* 2019; 290: 165-6.
16. MAKSYMOWYCH WP, LAMBERT RG, ØSTERGAARD M *et al.*: MRI lesions in the sacroiliac joints of patients with spondyloarthritis: an update of definitions and validation by the ASAS MRI working group. *Ann Rheum Dis* 2019; 78: 1550-8.
17. BARALIAKOS X, RICHTER A, FELDMANN D *et al.*: Frequency of MRI changes suggestive of axial spondyloarthritis in the axial skeleton in a large population-based cohort of individuals aged <45 years. *Ann Rheum Dis* 2020; 79: 186-92.
18. BARALIAKOS X, HELDMANN F, CALLHOFF J *et al.*: Which spinal lesions are associated with new bone formation in patients with ankylosing spondylitis treated with anti-TNF agents? A long-term observational study using MRI and conventional radiography. *Ann Rheum Dis* 2014; 73: 1819-25.
19. GUGGENBERGER R, GNANNT R, HODLER J *et al.*: Diagnostic performance of dual-energy CT for the detection of traumatic bone marrow lesions in the ankle: comparison with MR imaging. *Radiology* 2012; 264: 164-73.
20. WANG CK, TSAI JM, CHUANG MT, WANG MT, HUANG KY, LIN RM: Bone marrow edema in vertebral compression fractures: detection with dual energy CT. *Radiology* 2013; 269: 525-33.
21. JOHNSON TR: Dual-energy CT: general principles. *AJR Am J Roentgenol* 2012; 199 (5 Suppl.): S3-S8.
22. CHOI HK, BURNS LC, SHOJANIA K *et al.*: Dual energy CT in gout: a prospective validation study. *Ann Rheum Dis* 2012; 71: 1466-71.
23. COMMITTEE UNS: Report of the United Nations Scientific Committee on Effects of Atomic Radiation to the General Assembly, 2000.
24. OUICHKA R, BOUDERRAOUI F, RAYNAL M *et al.*: Performance of 18F-sodium fluoride positron emission tomography with computed tomography to assess inflammatory and structural sacroiliitis on magnetic resonance imaging in axial spondyloarthritis. *Clin Exp Rheumatol* 2019; 37: 19-25.
25. ESATOGLU SN, HATEMI G: Bone marrow oedema on sacroiliac/spine MRI: is it really a sign of objective inflammation warranting treatment?. *Clin Exp Rheumatol* 2019; 37 Suppl. 122: 10.